Heat and Mass Transfer of an Electrically Conducting Tangent Hyperbolic Fluid in the presence of thermal dispersion past a Stretching Surface

Gangadhar K.[1], Anselm O. Oyem[2] and Uma Maheswara K. Rao[3]
[1]Department of Mathematics, Acharya Nagarjuna University, Ongole, Andhra Pradesh -523001, India
[2]Department of Mathematics and Statistics, Islamic University in Uganda, P.O. Box 2555, Mbale, Uganda
[3]Department of Mathematics, Hyderabad Institute of Technology and Management, Gowdavelly Village, Rangareddy District, Hyderabad, Telangana 501401

Corresponding Author: anselmoyemfulokoja@gmail.com, onyekachukwu.oyem@fulokoja.edu.ng

Abstract

This study presents a steady, two dimensional, incompressible heat and mass transfer flow of an electrically conducting tangent hyperbolic fluid in the presence of thermal dispersion induced by a stretching surface. The governing partial differential equations, using similarity variables are transformed to a set of coupled nonlinear ordinary differential equations. The dimensionless results were obtained for velocity, temperature and concentration profiles and presented graphically. The obtained results shows that Weissenberg number increases with decrease in velocity profiles as thermophoresis effect increases with increase in concentration profiles.

Keywords: Stretching sheet; hyperbolic fluid; thermal dispersion; Weissenberg number

Nomenclature

k - Thermal conductivity (W/m K)
c_p – Specific heat at constant pressure (*J/kg K*)
f – Dimensionless stream function
u - Velocity component in x-direction (*m/s*)
v - Velocity component in y-direction (*m/s*)
$\alpha_e = \alpha_m + \gamma\, du$ - Effective thermal diffusivity
α_m - Molecular thermal diffusivity
γ - Mechanical thermal dispersion coefficient
d - Polar diameter
x – Cartesian coordinate (*m*)
T - Temperature of the fluid (^0C)
T_w - Temperature at the stretching surface
T_∞ - Ambient fluid temperature
$u_w(x)$ - Stretching velocity
i – Time index during navigation
L – Scale
Le – Lewis number
t – Time
N – Number of grid points
n – Power law index
We - Weissenberg number
M - Hartmann number
Ds - Thermal dispersion parameter

Sc - Schmidt number
Pr – Prandtl number
Re_x - Local Reynolds number
C_{fx} - Skin friction coefficient
Nu_x - Local Nusselt number
Nu_x - Local Nusselt number
Sh_x - Local Sherwood number
q_w - Surface heat flux
J_w - Surface mass flux
C - Concentration of the fluid
C_∞ – Ambient concentration
C_w - Concentration at the stretching surface

Greek symbols
α - Thermal diffusivity (m^2/s)
μ - Thermal viscosity ($N\ s/m$)
ρ - Fluid density (kg/m^3)
τ_w - Wall shear stress
ϕ – Dimensionless concentration
η – Similarity variable
$\upsilon = \dfrac{\mu}{\rho}$ - Kinematic viscosity of the fluid
μ_o – Zero shear rate viscosity
μ_∞ – Infinite shear rate viscosity
Γ – Time dependent material constant
θ - Non-dimensional temperature

Subscript
w – Condition at the surface
∞ - Condition at infinity

Superscript
$'$ - Differentiation with respect to η

Introduction
Study on electrically conducting non-Newtonian power-law fluid has have been carried out by a number of researchers due to its importance in the science and technology, engineering and industries for example, metallurgical processes, cooling of filaments, heat transfer properties, plastic and rubber sheet manufacturing, extrusion of polymers, blowing, floating or spinning of fibers, heat transfer, drawing stretching sheets through quiescent fluids, etc. Wang and Mujumdar [1] investigated on non-Newtonian fluids for mixed convection heat transfer from a vertical plate. Xu and Jan [2] studied the laminar boundary layer flow and heat and mass transfer analysis of non-Newtonian fluids past a stretching flat sheet. Xu *et al*. [3] researched on the series solutions of unsteady boundary layer flows of non-Newtonian fluids near a forward stagnation point. Megahed [4] investigated the boundary layer flow and heat transfer of a non-Newtonian power-law fluid over a non-linearly stretching vertical surface with heat fluid and thermal radiation. Abel

et al. [5] studied the boundary layer flow and heat transfer in a power-law fluid through a stretching sheet with variable thermal conductivity and non-uniform effects. Bilal *et al*. [6] discussed the mixed convection flow of Jeffrey nano-fluid over a radially stretching surface with thermal radiation effect. Wei and Al-Ashhab [7] studied the boundary layer flow of power-law non-Newtonian fluids with a novel boundary condition. The heat transfer mechanism and the constitutive models for energy boundary layer in power-law fluids were studied by Zheng and Zhang [8]. While, an analytical solution for boundary layer flow and heat transfer of non-Newtonian fluids in a porous media on an isothermal semi-infinite plate was studied by Wang and Tu [9]. Hady [10] analyzed the influence of laminar mixed convection flow of non-Newtonian fluids along a horizontal plate for uniform wall temperature. As Gorla [11] studied the effects of boundary induced streamwise pressure a gradient on laminar forced convection flow of heat transfer to non-Newtonian fluids from a horizontal plate. Mostafa [12] presented the slip effect on non-Newtonian power-law fluid past a continuously moving surface with suction using shooting method.

An important branch of the non-Newtonian fluid models is the hyperbolic tangent fluid model, used extensively for different laboratory experiments. From literature, Friedman *et al*. [13] studied the hyperbolic tangent fluid model for large-scale magneto-rheological fluid damper coils. Nadeem and Akram [14] researched on peristaltic transport of a hyperbolic tangent fluid model in an asymmetric channel. They further investigated the effects of partial slip on the peristaltic transport of a hyperbolic tangent fluid model in an asymmetric channel [15]. Natural convection boundary layer flow of a hyperbolic tangent fluid flowing past a vertical exponential circular cylinder with heat transfer analysis was studied by Naseer *et al*. [16].

The above literatures were restricted to MHD flows and mass transfer problems. Analysis of heat and mass transfer of a viscoelastic, electrically conducting fluid past a continuous stretching sheet was investigated by Kelly *et al*. [17]. Vajravelu *et al*. [18] investigated the effects of velocity slip, temperature and concentration jump conditions on MHD peristaltic transport of a Carreau fluid in a non-uniform channel. Jayachandra and Sandeep [19] investigated the effects of cross diffusion and MHD on non-Newtonian fluid flow over a slandering stretching sheet. Effect of MHD and heat transfer effects on a boundary layer flow of power-law non-Newtonian nanofluid over a vertical stretching sheet was looked into by Ferdows and Hamad [20]. Satyanarayana and Harish [21] studied the effects of chemical reaction, thermal radiation and MHD on heat and mass transfer of a Jeffrey fluid over a stretching sheet. Kasim and Mohammad [22] studied the effects of thermal stratification, heat source, MHD, Hall current and chemical reaction on heat and mass transfer over an unsteady stretching surface. Rushi [23] investigated the effects of magnetohydrodynamic and velocity slips on a flow, heat and mass transfer over a stretching sheet. Soret and Dufour effects on MHD convective radiative heat and mass transfer of nanofluids over a vertical non-linear stretching/shrinking sheet were investigated by Pal *et al*. [24]. Similarity solution of the boundary layer equations describing heat flow in a non-Newtonian power-law fluid by a continuously moving surface with a parallel free stream subject to MHD was examined by Kumari and Nath [25]. Akbar *et al*. [26] investigated the boundary layer flow of magnetohydrodynamic tangent hyperbolic fluid past a stretching sheet. Salahuddin *et al*. [27] studied the tangent hyperbolic fluid with exponentially varying viscosity in the presence of transverse magnetic field. Mekheimer *et al*. [28] investigated the peristaltic flow due to wavy moving wall of a two dimensional viscous fluid. He further discussed the effects of Hall current, MHD and slip condition due to a surface acoustic wavy wall in a porous medium [29]. Similarly, he investigated the boundary layer flow of heat and mass transfer on the peristaltic motion of second order fluid in a channel in the presence of magnetic field [30]. Salem and Rania [31] studied the effects of MHD, thermal radiation on a boundary layer flow of heat and mass transfer near a stagnation point over a stretching sheet embedded in a porous medium. They further investigated the thermal radiation and MHD effects on mixed convective boundary layer flow past a stretching sheet with variable viscosity [32].

The effects of heat and mass transfer fluids in a stretching sheet had not been adequately dealt with. Hence this present study which looks into the effects of heat and mass transfer of magnetic tangent hyperbolic fluid over a stretching sheet in the presence of thermal dispersion.

Mathematical Formulation

Consider a two-dimensional, steady, incompressible electrically conducting tangent hyperbolic fluid past a stretching surface, at $y = 0$ and $y > 0$. The equation of tangent hyperbolic fluid is given as [26]:

$$\bar{\tau} = \left[\mu_\infty + (\mu_0 + \mu_\infty) \tanh\left(\Gamma \bar{\dot{\gamma}}\right)^n \right] \bar{\dot{\gamma}} \quad (1)$$

where $\bar{\tau}$ is the extra stress tensor, μ_∞ is the infinite shear rate viscosity, μ_0 is the zero shear rate viscosity, Γ is the time dependent material constant, n is the power law index and $\bar{\dot{\gamma}}$ is the differential Mechanical thermal dispersion coefficient. The coefficient is defined by

$$\bar{\dot{\gamma}} = \sqrt{\frac{1}{2}\sum_i \sum_j \bar{\dot{\gamma}}_{ij}\ \bar{\dot{\gamma}}_{ji}} = \sqrt{\frac{1}{2}\Pi} \quad (2)$$

where $\Pi = \frac{1}{2} tr\left(grad\, V + (grad\, V)^T\right)^2$. Considering equation (1) at $\mu_\infty = 0$ and $\Gamma \bar{\dot{\gamma}} < 1$, it becomes

$$\bar{\tau} = \mu_0 \left[\left(\Gamma \bar{\dot{\gamma}}\right)^n \right] \bar{\dot{\gamma}} = \mu_0 \left[\left(1 + \Gamma \bar{\dot{\gamma}} - 1\right)^n \right] \bar{\dot{\gamma}} = \mu_0 \left[\left(1 + n\,(\Gamma \bar{\dot{\gamma}} - 1)\right) \right] \bar{\dot{\gamma}} \quad (3)$$

with external force f as:

$$f = J \times B \quad (4)$$

where $J = \sigma_0 \left(E + V \times B\right)$ is the current density, $B = (0, B_0)$ is the transverse uniform magnetic field applied to the fluid layer, σ_0 and E are the electric conductivity and the electric field respectively. For a very small Reynolds number, we assume the external electric field to be zero and the induced magnetic field is negligible. Thus, based on the assumptions taken, the governing partial differential equations are given as:

$$\frac{\partial u}{\partial x} + \frac{\partial v}{\partial y} = 0 \quad (5)$$

$$u\frac{\partial u}{\partial x} + v\frac{\partial u}{\partial y} = \upsilon (1-n)\frac{\partial^2 u}{\partial y^2} + \sqrt{2}\upsilon n\, \Gamma \left(\frac{\partial u}{\partial y}\right)\frac{\partial^2 u}{\partial y^2} - \frac{\sigma B_0^2}{\rho} u \quad (6)$$

$$u\frac{\partial T}{\partial x} + v\frac{\partial T}{\partial y} = \frac{\partial}{\partial y}\left(\alpha_e \frac{\partial T}{\partial y}\right) \quad (7)$$

$$u\frac{\partial C}{\partial x} + v\frac{\partial C}{\partial y} = D\frac{\partial^2 C}{\partial y^2} \quad (8)$$

subject to the boundary conditions

$$y = 0 : u = u_w(x) = ax, v = 0, T = T_w, C = C_w \tag{9}$$

$$y \to \infty : u \to 0, T \to T_\infty, C \to C_\infty \tag{10}$$

Equations (5) – (10) are transformed by introducing the stream function $\psi(x, y)$ and the following similarity variables:

$$\begin{aligned} &u = axf'(\eta), \quad v = -\sqrt{a\upsilon}\, f(\eta), \quad \eta = \sqrt{\frac{a}{\upsilon}}y, \\ &\theta(\eta) = \frac{T - T_\infty}{T_w - T_\infty}, \quad \phi(\eta) = \frac{C - C_\infty}{C_w - C_\infty} \end{aligned} \tag{11}$$

Applying equation (11), equation (5) is satisfied and equations (6) – (10) reduce to the following dimensionless coupled nonlinear ordinary differential equations

$$(1-n) f''' + ff'' - f'^2 + nWe\ f'''(f'') - Mf' = 0 \tag{12}$$

$$\theta''(1 + Dsf') + Ds\theta' f'' + \Pr f\theta' = 0 \tag{13}$$

$$\phi'' + Scf\phi' = 0 \tag{14}$$

with ordinary boundary conditions

$$f(0) = 0, \quad f'(0) = 1, \quad \theta(0) = 1, \quad \phi(0) = 1 \tag{15}$$

$$f'(\infty) = 0, \quad \theta(\infty) = 0, \quad \phi(\infty) = 0 \tag{16}$$

where prime denotes differentiation with respect to η and Weissenberg number, Prandtl number, Hartmann number, thermal dispersion parameter and Schmidt number Sc are defined by;

$$We = \frac{\sqrt{2}a^{\frac{3}{2}}x\Gamma}{\sqrt{\upsilon}}, \ \Pr = \frac{\upsilon}{\alpha}, \ M = \frac{\sigma B_0^2}{\rho a}, \ Ds = \frac{\gamma du_w}{\alpha_m}, \ Sc = \frac{\alpha}{D} \tag{17}$$

The shear stress at the surface of the wall τ_w is given by:

$$\tau_w = \left[(1-n)\frac{\partial u}{\partial y} + \frac{n\Gamma}{\sqrt{2}}\left(\frac{\partial u}{\partial y}\right)^2 \right]_{y=0} \tag{18}$$

where μ is the coefficient of viscosity. The skin friction coefficient is defined by

$$C_f = \frac{\tau_w}{\rho u_w^2} \tag{19}$$

using equations (17) and (18) we obtain the dimensionless skin friction coefficient as

$$C_{fx}\,\mathrm{Re}_x^{1/2} = \left[(1-n) f''(0) + \frac{n}{2} We \left(f''(0) \right)^2 \right] \tag{20}$$

Similarly, the heat transfer rate at the wall is given by

$$q_w = -k\left(\frac{\partial T}{\partial y}\right)_{y=0} \tag{21}$$

where k is the thermal conductivity of the fluid and the Nusselt number is defined by

$$Nu_x = \frac{x}{k}\frac{q_w}{T_w - T_\infty} \tag{22}$$

Thus, using equations (17) and (21) in (22) the dimensionless heat transfer rate is given as

$$\frac{Nu_x}{\mathrm{Re}_x^{1/2}} = -\theta'(0) \tag{23}$$

Similarly, the mass flux and Sherwood number are defined as:

$$J_w = -D\left(\frac{\partial C}{\partial y}\right)_{y=0} \tag{24}$$

$$Sh_x = \frac{x}{D}\frac{J_w}{C_w - C_\infty} \tag{25}$$

Using equation (17) and (24) in (25) the dimensionless wall mass transfer rate is obtained as:

$$\frac{Sh_x}{\mathrm{Re}_x^{1/2}} = -\phi'(0) \tag{26}$$

where $\mathrm{Re}_x = \frac{xu_w(x)}{\upsilon}$ represents the local Reynolds number.

Solution of the Problem

The Spectral Relaxation Method (SRM) is employed to solve the coupled nonlinear ordinary differential equations (12) – (14) subject to the boundary conditions (15) and (16) by first, discretizing the differential equations (12) – (16) using the Chebyshev Spectral Collocation Methods (CSCM) [34,35] and obtains;

$$f'_{r+1} = p_r,\ f_{r+1}(0) = 0 \tag{27}$$

$$p''_{r+1} + (nWe\,p' - n)p'_{r+1} + (f_{r+1})p_{r+1} - Mp_{r+1} = p_r^2 \tag{28}$$

$$\theta''_{r+1}(1 + Ds\,p_{r+1}) + (Ds\,p'_{r+1} + \mathrm{Pr}\,f_{r+1})\theta'_{r+1} = 0 \tag{29}$$

$$\phi''_{r+1} + Sc\,(f_{r+1})\phi'_{r+1} = 0 \tag{30}$$

with iterated conditions

$$p_{r+1}(0) = 1, \quad \theta_{r+1}(0) = 1, \quad \phi_{r+1}(0) = 1 \tag{31}$$

$$p_{r+1}(\infty)=0, \quad \theta_{r+1}(\infty)=0, \quad \phi_{r+1}(\infty)=0 \tag{32}$$

using $\eta = L(\xi+1)/2$ with computational domain $[0, L]$ in equations (27) – (30), we obtain the interval $[-1, 1]$. Introducing a differentiation matrix D, we approximate the derivatives of the unknown variables at the collocation points as:

$$\frac{\partial f_{r+1}}{\partial \eta} = \sum_{k=0}^{\bar{N}} D_{lk} f_r(\xi_k) = Df_r, \quad l = 0, 1, 2, \cdots, \bar{N}+1 \tag{33}$$

where $\bar{N}+1$ is the number of collocation points (grid points), $D = 2D/L$ and $f = \left[f(\xi_0), f(\xi_1), f(\xi_2), \cdots, f(\xi_{\bar{N}})\right]^T$ are the vector functions at the collocation points. For higher-order derivatives of D, we have;

$$f_r^{(p)} = D^p f_r \tag{34}$$

where p is the order of the derivative. Applying the Spectral Relaxation Method (SRM) to equations (27) – (30), we obtain

$$A_1 f_{r+1} = B_1, \qquad f_{r+1}(\xi_{\bar{N}}) = 0 \tag{35}$$

$$A_2 p_{r+1} = B_2, \quad p_{r+1}(\xi_{\bar{N}}) = 1, \quad p_{r+1}(\xi_0) = 0 \tag{36}$$

$$A_3 \theta_{r+1} = B_3, \quad \theta_{r+1}(\xi_{\bar{N}}) = 1, \quad \theta_{r+1}(\xi_0) = 0 \tag{37}$$

$$A_4 \phi_{r+1} = B_4, \quad \phi_{r+1}(\xi_{\bar{N}}) = 1, \quad \phi_{r+1}(\xi_0) = 0 \tag{38}$$

where,

$$A_1 = D, \quad B_1 = p_r \tag{39}$$

$$A_2 = D^2 + diag\left(nWep'_{r+1} - n\right)D^2 + diag\left(f_{r+1}\right)D - MI, \quad B_2 = p_r^2 \tag{40}$$

$$A_3 = diag(1 + Dsp_{r+1})D^2 + diag\left(\Pr f_{r+1} + Dsp'_{r+1}\right)D, \quad B_3 = 0 \tag{41}$$

$$A_4 = D^2 + diag\left(Scf_{r+1}\right)D, \quad B_4 = 0 \tag{42}$$

where I is an identity matrix, $diag(\cdot)$ is a diagonal matrix, $\bar{N}$ is the number of grid points, f, p, θ and ϕ are the values of the functions respectively when evaluated at the grid points and the subscript r denotes the iteration number. Let the initial guesses for the SRM scheme be

$$f_0(\eta) = 1 - e^{-\eta}, \quad p_0(\eta) = e^{-\eta}, \quad \theta_0(\eta) = e^{-\eta}, \quad \phi_0(\eta) = e^{-\eta} \tag{43}$$

equations (43) are chosen to satisfy the boundary conditions until convergence is achieved defined as

$$Er = Max\left(\left\| f_{r+1} - f_r \right\|, \quad \left\| p_{r+1} - p_r \right\|, \quad \left\| \theta_{r+1} - \theta_r \right\|, \quad \left\| \phi_{r+1} - \phi_r \right\|\right) \tag{44}$$

Results and Discussion

A steady heat and mass transfer of electrically conducting tangent hyperbolic fluid past a stretching sheet in the presence of thermal dispersion have been considered. The partial differential equations (5) – (8) subject to the boundary conditions (9) and (10) were transformed to a set of coupled nonlinear ordinary differential equations (12) – (14) subject to the conditions (15) and (16). These set of coupled nonlinear equations (12) – (16) were solved numerically using the Spectral Relaxation Method (SRM) with accuracy at $\eta_\infty = 15$ and grid points $\overline{N} = 100$ for selected values of the governing parameters. This was implemented using Matlab and the parameter effects on velocity, temperature and concentration profiles are displayed graphically in figures 2 – 14. While the numerical results for the skin friction coefficient, Nusselt and Sherwood number are presented in tables 1 – 4.

Figures 2 – 10 displays the effects of power law index, Weissenberg number and Hartmann number on velocity, temperature and concentrations profiles., it was observed that velocity profiles decreases with increasing values in n, We and M but increases in both temperature an concentration profiles respectively as n, We and M increases. Prandtl number is the ratio of momentum diffusivity (kinematic viscosity) to thermal diffusivity. Thus, increasing the values of Prandtl number, the momentum diffusivity will dominate thermal diffusivity. Figure 11 and 12 shows the effects of $\Pr$ on temperature and concentration profiles. It was observed that increase in $\Pr$ results in the decrease in temperature and concentration profiles along the stretching wall towards the free stream.

Figure 13 shows the effects of thermal dispersion Ds on temperature profiles. It was observed that temperature profiles increases gradually away from the wall towards the free stream as Ds increases in value. Thereby enhancing the transport of heat along the stretching sheet and this is useful in showing that, the use of fluid medium with better heat dispersion properties result in better heat transfer characteristics that may be required in many industrial applications such as packed bed reactors, nuclear waste disposal, etc. figure 14 shows the effects of Schmidt number on concentration profiles. Schmidt number Sc is the ratio of momentum diffusivity (viscosity) and mass diffusivity. It was observed in figure 14 that concentration profiles decreases along the wall towards the free stream as *Sc* increases.

The numerical values of skin friction coefficient, Nusselt number and Sherwood number for some governing parameters are presented in tables 1 - 3. It was observed in table 1 that power law index n and Weissenberg number We increases as skin friction coefficient C_{fx} decreases, but increases with increasing values in M with an average number of iteration of 27 for SRM and 15 for SRM with Successive Over-Relaxation (SOR) technique. Similarly, Nusselt number increases with increasing values in $\Pr$ but decreases with increasing values in n, We, M and Ds as shown in table 2. From table 3, Sherwood number decreases with increasing values in n, We, M and Sc. A comparison of the present study in term of skin-friction coefficient with Akbar *et al*. [26] for different values of power law and Weissenberg number when $\Pr = Sc = Ds = M = 0$ is presented in table 4. It was observed that the present results are in agreement with the earlier findings of [26].

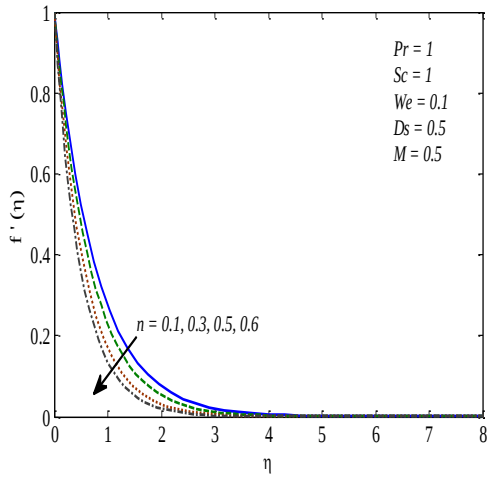

Figure 2: Velocity profiles for various values of n

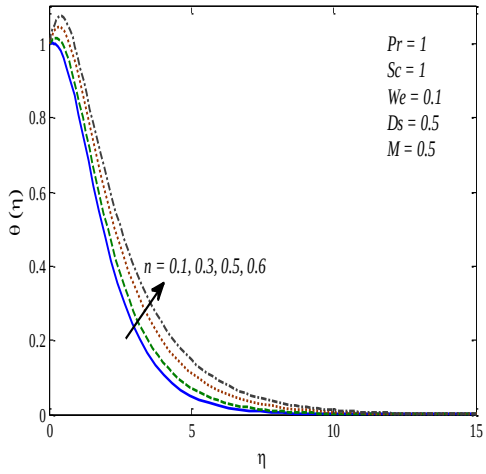

Figure 3: Temperature profile for various values of n

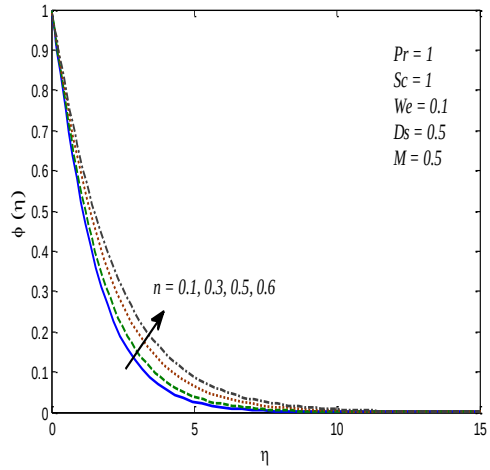

Figure 4: Concentration profile for different values of n

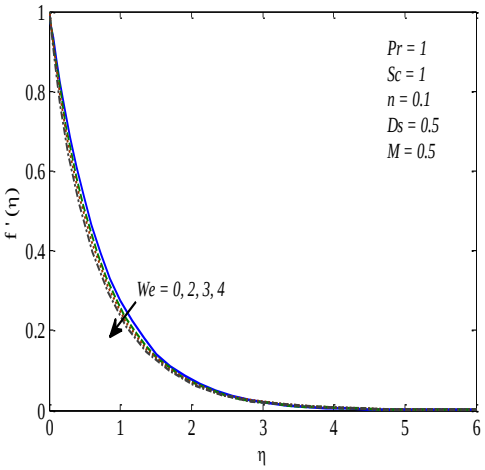

Figure 5: Velocity profile for different values of We

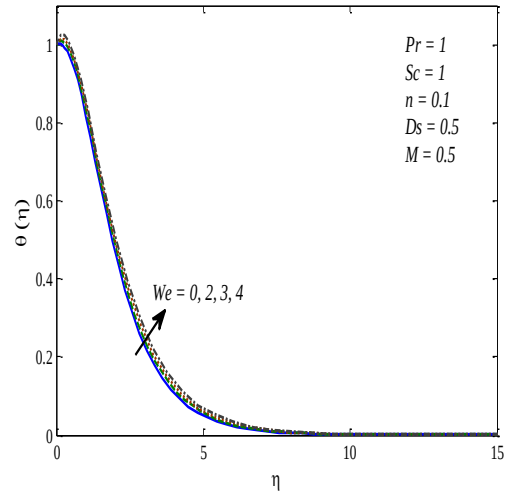

Figure 6: Temperature profile for different values of We

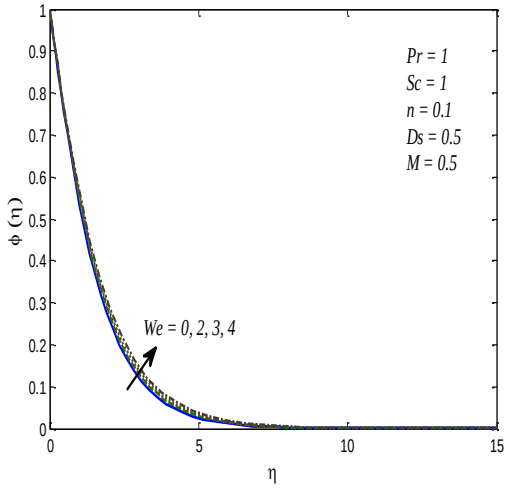

Figure 7: Concentration profile for different values of We

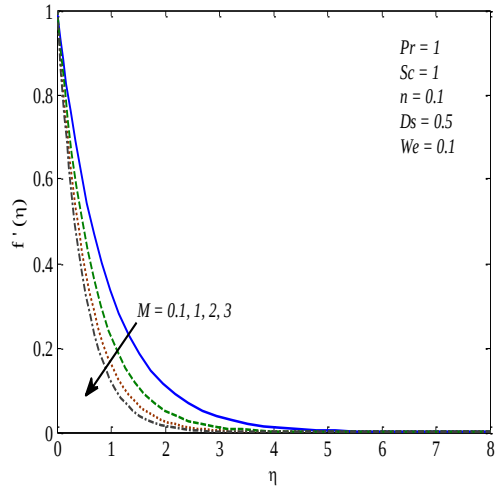

Figure 8: Velocity profile for different values of M

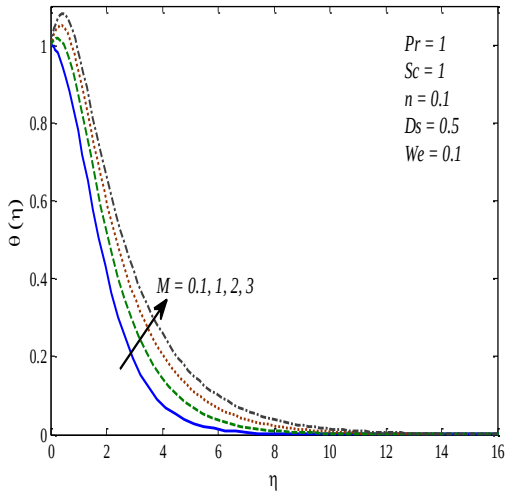

Figure 9: Temperature profile for different values of M

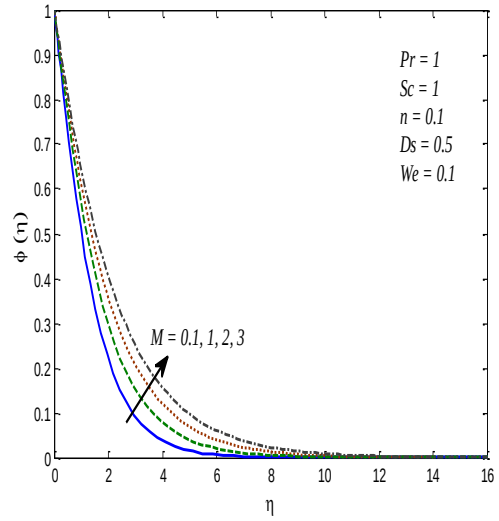

Figure 10: Concentration profile for different values of M

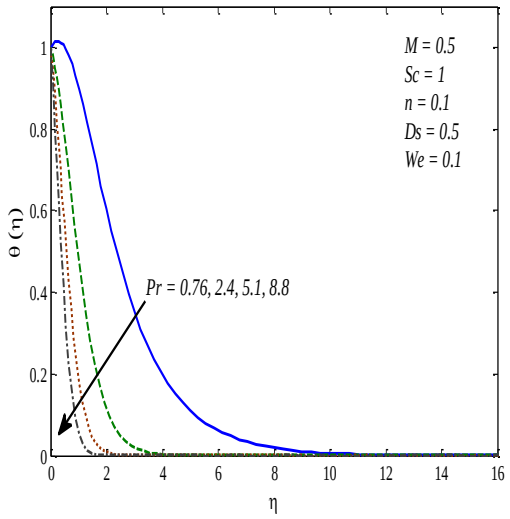

Figure 11: Temperature profile for different values of $\Pr$

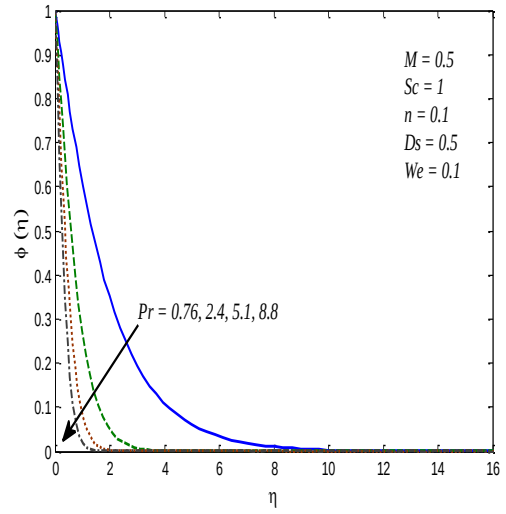

Figure 12: Concentration profile for different values of $\Pr$

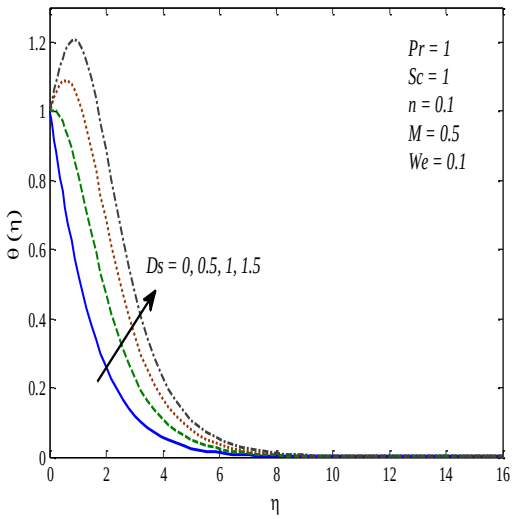

Figure 13: Temperature profilefor different values of Ds

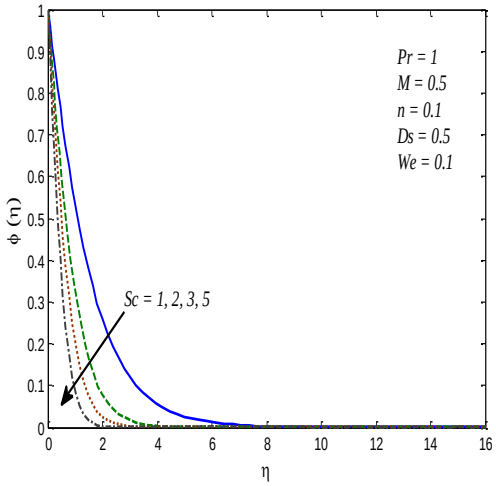

Figure 14: Concentration profile $\phi(\eta)$ for different values of Sc

Table 1: Numerical values for magnitude of $\sqrt{\mathrm{Re}_x}C_{fx}$ at the surface for different values of $n,\ We\ and\ M$ with $\mathrm{Pr} = Sc = 3, Ds = 0.5$

n	We	M	Iter	Basic SRM	Iter	SRM with SOR	$\sqrt{\mathrm{Re}_x}C_{fx}$
0.1	0.1	0.5	27	1.15892610	15	1.15892610	1.15892610
0.2	0.1	0.5	27	1.08871946	15	1.08871946	1.08871946
0.3	0.1	0.5	28	1.01304949	15	1.01304949	1.01304949
0.4	0.1	0.5	27	0.93028371	16	0.93028371	0.93028371
0.5	0.1	0.5	27	0.83768770	16	0.83768770	0.83768770
0.1	0.5	0.5	27	1.14675023	15	1.14675023	1.14675023
0.1	1.0	0.5	27	1.13077992	15	1.13077992	1.13077992
0.1	1.5	0.5	26	1.11383010	15	1.11383010	1.11383010
0.1	2.0	0.5	25	1.09568709	15	1.09568709	1.09568709
0.1	0.1	1.0	20	1.33774497	15	1.33774497	1.33774497
0.1	0.1	1.5	16	1.49517344	12	1.49517344	1.49517344
0.1	0.1	2.0	15	1.63740820	11	1.63740820	1.63740820
0.1	0.1	2.5	14	1.76813004	11	1.76813004	1.76813004

Table 2: Numerical values for $-\theta'(0)$ at the surface for $n, We, M, Ds\ and\ \mathrm{Pr}$ for $Sc = 3\,i$

n	We	M	Ds	Pr	Iter	Basic SRM	Iter	SRM with SOR	$-\theta'(0)$
0.1	0.1	0.5	0.5	3	27	0.34830914	15	0.34830914	0.34830914
0.2	0.1	0.5	0.5	3	27	0.30469477	15	0.30469477	0.30469477
0.3	0.1	0.5	0.5	3	28	0.25143371	15	0.25143371	0.25143371
0.4	0.1	0.5	0.5	3	27	0.18377463	16	0.18377463	0.18377463
0.5	0.1	0.5	0.5	3	27	0.09225247	16	0.09225247	0.09225247
0.1	0.5	0.5	0.5	3	27	0.33725987	15	0.33725987	0.33725987
0.1	1.0	0.5	0.5	3	27	0.32193450	15	0.32193450	0.32193450
0.1	1.5	0.5	0.5	3	26	0.30445542	15	0.30445542	0.30445542
0.1	2.0	0.5	0.5	3	25	0.28404527	15	0.28404527	0.28404527
0.1	0.1	1.0	0.5	3	20	0.24781975	15	0.24781975	0.24781975
0.1	0.1	1.5	0.5	3	16	0.16275842	12	0.16275842	0.16275842
0.1	0.1	2.0	0.5	3	15	0.08840660	11	0.08840660	0.08840660
0.1	0.1	2.5	0.5	3	14	0.02199313	11	0.02199313	0.02199313
0.1	0.1	0.5	0.6	3	27	0.26010269	15	0.26010269	0.26010269
0.1	0.1	0.5	0.7	3	27	0.18384194	15	0.18384194	0.18384194
0.1	0.1	0.5	0.9	3	27	0.05926624	15	0.05926624	0.05926624
0.1	0.1	0.5	1.0	3	27	0.00800780	15	0.00800780	0.00800780
0.1	0.1	0.5	0.5	4	27	0.50654478	15	0.50654478	0.50654478
0.1	0.1	0.5	0.5	5	27	0.64876889	15	0.64876889	0.64876889
0.1	0.1	0.5	0.5	6	27	0.77905057	15	0.77905057	0.77905057

0.1	0.1	0.5	0.5	7	27	0.89997906	15	0.89997906	0.89997906

Table 3: Numerical values for $-\phi'(0)$ at the surface for $n, We, M, \Pr$ *and* Sc

n	We	M	Sc	Iter	SRM	Iter	SRM with SOR	$-\phi'(0)$
0.1	0.1	0.5	3	27	1.14994911	15	1.14994911	1.14994911
0.2	0.1	0.5	3	27	1.15822671	15	1.15822671	1.15822671
0.3	0.1	0.5	3	28	1.16903669	15	1.16903669	1.16903669
0.4	0.1	0.5	3	27	1.18411251	16	1.18411251	1.18411251
0.5	0.1	0.5	3	27	1.20747627	16	1.20747627	1.20747627
0.1	0.5	0.5	3	27	1.15363168	15	1.15363168	1.15363168
0.1	1.0	0.5	3	27	1.15899953	15	1.15899953	1.15899953
0.1	1.5	0.5	3	26	1.16550175	15	1.16550175	1.16550175
0.1	2.0	0.5	3	25	1.17362208	15	1.17362208	1.17362208
0.1	0.1	1.0	3	20	1.16799112	15	1.16799112	1.16799112
0.1	0.1	1.5	3	16	1.18443863	12	1.18443863	1.18443863
0.1	0.1	2.0	3	15	1.19988301	11	1.19988301	1.19988301
0.1	0.1	2.5	3	14	1.21465515	11	1.21465515	1.21465515
0.1	0.1	0.5	4	27	1.31034052	15	1.31034052	1.31034052
0.1	0.1	0.5	5	27	1.45177799	15	1.45177799	1.45177799
0.1	0.1	0.5	6	27	1.57968243	15	1.57968243	1.57968243
0.1	0.1	0.5	7	27	1.69730903	15	1.69730903	1.69730903

Table 4: Comparison of Skin-friction coefficient $\sqrt{\mathrm{Re}_x}C_{fx}$ with the available results in literature for different values of n *and* We when $\Pr = Sc = Ds = M = 0$

	$\sqrt{\mathrm{Re}_x}C_{fx}$					
	$We = 0.0$		$We = 0.3$		$We = 0.5$	
n	Present study	Akbar et al. [26]	Present study	Akbar et al. [26]	Present study	Akbar et al. [26]
0.0	1.00000000	1.00000	1.00000000	1.00000	1.00000000	1.00000
0.1	0.94868330	0.94868	0.94247918	0.94248	0.93825864	0.93826
0.2	0.89442719	0.89442	0.88022646	0.88023	0.87026055	0.87026

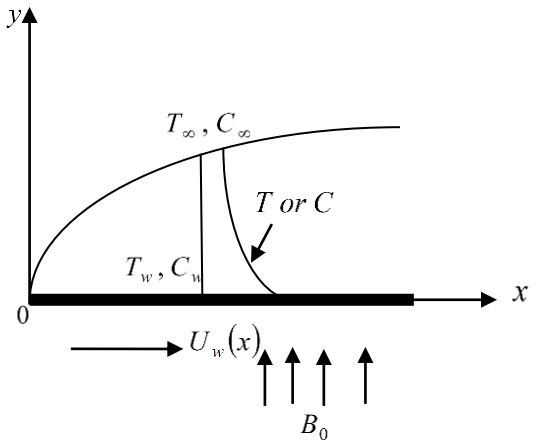

Fig. 1. Schematic diagram of the problem

Conclusion

In this study we considered a Spectral Relaxation Method to heat and mass transfer flow in MHD tangent hyperbolic fluid flow over stretching sheet in the presence of thermal dispersion. On applying the SRM to equations (35) – (42), the following are observed;

i). That velocity profiles decreases with increase in $\Pr$, We and n

ii). That temperature and concentration profiles increases with increase in Ds , We and n , but decreases with Pr and Sc.

iii). That thermal dispersion parameter has a strong influence over the temperature profiles.

iv). That SRM significantly improved in conjunction with the SOR method with $\omega = 1$

Acknowledgements

The authors would like to thank Gangadhar for his consistent mentoring towards the success of this article.

References:

Wang X.Q., Mujumdar A.S., (2007). Heat transfer characteristics of nano-fluids: a review. *International Journal of Thermal Science*, 46, 1–19.

Xu H., Jun L.S., (2009). Laminar flow and heat transfer in the boundary-layer of non-Newtonian fluids over a stretching flat sheet. *Computers and Mathematics with Applications*, 57 (9), 1425–1431.

Xu H., Liao S.J., Pop I., (2006). Series solution of unsteady boundary layer flows of non-Newtonian fluids near a forward stagnation point. *Journal of Non-Newtonian Fluid Mechanics*, 139, 31–43.

Megahed A.M., (2015). Flow and heat transfer of a non-Newtonian power–law fluid over a non-linearly stretching vertical surface with heat flux and thermal radiation. *Mechanica*, 50 (7), 1693–1700.

Abel M.S., Datti P.S., Mahesha N., (2009). Flow and heat transfer in a power-law fluid over a stretching sheet with variable thermal conductivity and non-uniform heat source. *International Journal of Heat and Mass Transfer*, 52(11–12), 2902–2913.

Bilal A.M., Hayat T., Alsaedi A., (2015). Convective heat and mass transfer in MHD mixed convection flow of Jeffrey nano-fluid over a radially stretching surface with thermal radiation. *Journal of Central South University*, 22(3), 1114–1123.

Wei D.M., Al-Ashhab S., (2014). Similarity solutions for non-Newtonian power-law fluid flow. *Applied Mathematics and Mechanics*, 35(9), 1155–1166.

Zheng L., Zhang X.J., (2008). On energy boundary layer equations in power law non-Newtonian fluids. *Journal of Central South University of Technology*, 15, 5–8.

Wang C., Tu C., (1989). Boundary-layer flow and heat transfer of non-Newtonian fluids in porous media. *International Journal of Heat and Fluid Flow*, 10(2), 160–165.

Hady F.M., (1995). Mixed convection boundary-layer flow of non-Newtonian fluids on a horizontal plate. *Applied Mathematics and Computation*, 68, 105–112.

Gorla R.S.R., (1986). Combined forced and free convection in boundary layer flow of non-Newtonian fluid on a horizontal plate. *Chemical Engineering Communications*, 49, 13–22.

Mostafa A.A.M., (2011). Slip velocity effect on a non-Newtonian power-law fluid over a moving permeable surface with heat generation. *Mathematical and Computer Modeling*, 54, 1228–1237.

Friedman A.J., Dyke S.J., Phillips B.M., (2013). Over-driven control for large-scale MR dampers. *Smart Materials and Structures*, 22, 15.

Nadeem S., Akram S., (2009). Peristaltic transport of a hyperbolic tangent fluid model in an asymmetric channel. *Zeitschrift für Naturforschung A.*, 64a, 559–567.

Nadeem S., Akram S., (2010). Effects of partial slip on the peristaltic transport of a hyperbolic tangent fluid model in an asymmetric channel. *International Journal for Numerical Methods in Fluids*, 63, 374–394.

Naseer M., Malik M.Y., Nadeem S., Rehman A., (2014). The boundary layer flow of hyperbolic tangent fluid over a vertical exponentially stretching cylinder. *Alexandria Engineering Journal*, 53, 747–750.

Kelly D., Vajravelu K., Andrews L., (1999). Analysis of heat and mass transfer of a viscoelastic, electrically conducting fluid past a continuous stretching sheet. *Nonlinear Analysis*, 36 (6), 767–784.

Vajravelu K., Sreenadh S., Saravana R., (2013). Combined influence of velocity slip, temperature and concentration jump conditions on MHD peristaltic transport of a Carreau fluid in a non-uniform channel. *Applied Mathematics and Computation*, 225, 656–676.

Jayachandra B.M., Sandeep N., (2016). MHD non-Newtonian fluid flow over a slendering stretching sheet in the presence of cross-diffusion effects. *Alexandria Engineering Journal*, 55, 2193–2201.

Ferdows M., Hamad M.A.A., (2016). MHD flow and heat transfer of a power–law non-Newtonian nano-fluid (Cu-H_2O) over a vertical stretching sheet. *Journal of Applied Mechanics and Technical Physics*, 57(4), 603–610.

Satyanarayana N.P.V., Harish B.D., (2016). Numerical study of MHD heat and mass transfer of a Jeffrey fluid over a stretching sheet with chemical reaction and thermal radiation. *Journal of the Taiwan Institute of Chemical Engineers*, 59, 18–25.

Kasim A., Mohammad A.R.M., (2012). Effect of thermal stratification on MHD free convection with heat and mass transfer over an unsteady stretching surface with heat source, Hall Current and chemical reaction. *International Journal of Advances in Engineering Science and Applied Mathematics*, 4(3), 217–225.

Rushi K.B., (2013). MHD boundary layer flow on heat and mass transfer over a stretching sheet with slip effect. *Journal of Naval Architecture and Marine Engineering*, 10, 16–26.

Pal D., Mandal G., Vajravelu K., (2016). Soret and Dufour effects on MHD convective-radiative heat and mass transfer of nano-fluids over a vertical non-linear stretching/shrinking sheet. *Applied Mathematics and Computations*, 287, 184–200.

Kumari M., Nath G., (2001). MHD boundary layer flow of a non-Newtonian fluid over a continuously moving surface with a parallel free stream. *Acta Mechanica*, 146(3), 139–150.

Akbar N.S., Nadeem S., Haq R.U., Khan Z.H., (2013). Numerical solutions of magnetohydrodynamic boundary layer flow of tangent hyperbolic fluid towards a stretching sheet. *Indian Journal of Physics*, 87 (11), 1121–1124.

Salahuddin T., Malik M.Y., Hussain A., Bilal S., Awais M., (2015). Effects of transverse magnetic field with variable thermal conductivity on tangent hyperbolic fluid with exponentially varying viscosity. *AIP Advances*, 5, 127–103.

Mekheimer Kh. S., Salem A.M., Zaher A.Z., (2013), Peristaltic induced flow due to a surface acoustic wavy moving wall. *Chines Journal of Physics*, 51 (5), 954–968.

Mekheimer Kh. S., Salem A.M., Zaher A.Z., (2013). Peristaltically induced MHD slip flow in a porous medium due to a surface acoustic wavy wall. *Journal of the Egyptian Mathematical Society*, 22(1), 143–151.

Mekheımer Kh. S., Najma S., Hayat T., (2012). Simultaneous effects of induced magnetic field and heat and mass transfer on the peristaltic motion of second-order fluid in a channel. *International Journal for Numerical Methods in Fluids*, 70, 342–358.

Salem A.M., Rania F., (2010). Effect of thermal radiation on MHD mixed convective heat transfer adjacent to a vertical continuously stretching sheet in the presence of variable viscosity. *Journal of the Korean physical society*. 57 (6), 1401–1407.

Salem A.M., Rania F., (2012). Effect of variable properties on MHD heat and mass transfer flow near a stagnation point towards a stretching sheet in a porous medium with thermal radiation. *Chinese Physics B.*, 21 (6), 1–11.

Motsa S.S., Makukula Z.G., (2013). On spectral relaxation method approach for steady von Karman flow of a Reiner-Rivlin fluid with Joule heating, viscous dissipation and suction/injection. *Cent. Eur. J. Phys.*, 11, 363–374.

Canuto C., Hussaini M.V., Quarteroni A., Zang T.A., (1988). Spectral Methods in Fluid Dynamics. Springer, Berlin.

Trefethen, L.N., (2000). Spectral Methods in MATLAB. SIAM, Philadelphia